

Article

A Maximum Efficiency Point Tracking Control Scheme Based on Different Cross Coupling of Dual-Receiver Inductive Power Transfer System

Ruikun Mai ¹, Linsen Ma ¹, Yeran Liu ¹, Pengfei Yue ¹, Guangzhong Cao ² and Zhengyou He ^{1,*}

¹ State Key Laboratory of Traction Power, Southwest Jiaotong University, Chengdu 610031, China; mairk@swjtu.cn (R.M.); marinse@163.com (L.M.); yeranliu@my.swjtu.edu.cn (Y.L.); yuepengfei_yf@163.com (P.Y.)

² Shenzhen Key Laboratory of Electromagnetic Control, College of Mechatronics and Control Engineering, Shenzhen University, Shenzhen 518060, China; gzcao@szu.edu.cn

* Correspondence: hezy@home.swjtu.edu.cn; Tel.: +86-28-8760-2445

Academic Editors: Sheldon S. Williamson, Akshay K. Rathore, Fei Gao, Ritesh Keshri, Jin Ye and Lalit Patnaik
Received: 15 October 2016; Accepted: 7 February 2017; Published: 13 February 2017

Abstract: One of the most promising inductive power transfer applications is the wireless power supply for locomotives which may cancel the need for pantographs. In order to meet the dynamic and high power demands of wireless power supplies for locomotives, a relatively long transmitter track and multiple receivers are usually adopted. However, during the dynamic charging, the mutual inductances between the transmitter and receivers vary and the load of the locomotives also changes randomly, which dramatically affects the system efficiency. A maximum efficiency point tracking control scheme is proposed to improve the system efficiency against the variation of the load and the mutual inductances between the transmitter and receivers while considering the cross coupling between receivers. Firstly, a detailed theoretical analysis on dual receivers is carried out. Then a control scheme with three control loops is proposed to regulate the receiver currents to be the same, to regulate the output voltage and to search for the maximum efficiency point. Finally, a 2 kW prototype is established to validate the performance of the proposed method. The overall system efficiency (DC-DC efficiency) reaches 90.6% at rated power and is improved by 5.8% with the proposed method under light load compared with the traditional constant output voltage control method.

Keywords: inductive power transfer; system efficiency improvement; maximum efficiency point tracking (MEPT); multiple-receiver

1. Introduction

In recent years, inductive power transfer (IPT) technology has made rapid progress [1,2]. As a promising technology, IPT technology can transfer energy over an air gap of a certain size via a high frequency magnetic field. IPT technology has been successfully applied in several low power applications, such as mobile phones [3], sensors [4] and so on. For high power applications (rail locomotives, electric cars, buses and other hybrid electric vehicles) [5,6], it is a huge challenge for the single-receiver IPT system to get enough power from the transmitter other than from multiple-receiver systems, which could dramatically increase the capacity of receiving power.

Generally, output power and system efficiency are two of the most important concerns for IPT systems. However, the limitation of semiconductor devices' capacity makes it hard for a traditional single-receiver IPT system to meet the heavy load demand. Therefore, the multiple-receiver approach may be a promising solution to meet the high power demands of railway charging applications. A long transmitter track is usually employed to generate high magnetic fields in IPT systems for railway

applications [7]. As the train body is normally long, parallel-connected multiple receivers could be mounted together side by side along the track to pick up the magnetic power to feed the load as shown in Figure 1. These parallel-connected receivers can pick up more power in total than a single receiver does without increasing the capacity of semiconductors.

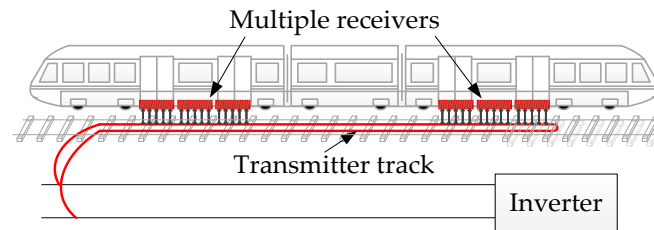


Figure 1. Transmitter track and multiple receivers in the wireless power supply system for railway applications.

Many researchers have paid attention to multiple-receiver IPT systems. The IPT system with dual secondary windings is analyzed in [8] and a general tuning method with any combination of secondary side compensation schemes is also proposed. The closed form for realizing maximum power transfer and maximum efficiency transfer of the IPT system, which adopted one transmitter and two receivers, is investigated in [9] and an optimal range of load resistance was determined accordingly. An equivalent model for any multiple-receiver system is given in [10] and the optimal load is analyzed.

The researches above are based on the assumption that the cross coupling between the multiple receivers are zero. However, receivers are placed very close to each other due to the limited available space of the train body. The cross coupling between receivers could have great influence on the adjacent one and should not be ignored. If cross coupling exists between the multiple receivers, the resonant frequency of the coupled receivers is changed [11] and the system efficiency also decreases accordingly [11,12].

In order to suppress the adversity of the cross coupling between the receivers, some methods have been proposed to improve the performance of IPT systems. An impedance matching method considering the cross coupling between the source coil and receivers is proposed and a design procedure for a single source coil and the optimal load impedance are presented in [13]. The operational frequency for maximum efficiency transfer under the cross coupling between receivers is illustrated by adjusting the operational frequency to tune the receivers in [11]. A load impedance matching algorithm is proposed in [14] to control power allocation between two receivers, so that system efficiency is improved. Additional inductive or capacitive reactance is employed to suppress the influence of cross coupling between receivers in [12].

The efficiency improvement methods for multiple-receiver IPT system mentioned above assume a constant optimal load value. However, the equivalent resistance of the load, for example, in a battery, can go from 3.6Ω to 560Ω depending on its charging profile [15]. As a result, it is hard for the system to work in the efficiency-optimized load range all the time. Some maximum efficiency point tracking (MEPT) methods for single-receiver IPT systems have been proposed [16]. A boost converter is employed in the secondary side to control the input voltage of the rectifier to maintain high efficiency in [17]. A DC/DC converter either on the primary side or the secondary side is applied to search for the maximum efficiency point by adjusting the duty cycle in [18,19]. In addition, an active rectifier can be applied to maintain constant the current ratio between the transmitter coil and receiver coils in order to optimize system efficiency without an additional DC/DC converter in [20].

From the discussion above, some progress has been made in the analysis and efficiency improvement of multiple-receiver IPT system in a static state, but there are two main problems

that need to be addressed for a practical high power multiple-receiver IPT system under dynamic conditions:

- (1) When the receivers move along the transmitter track, the relative positions between the receivers and the transmitter track change from time to time. Therefore, the induced voltage on each receiver coil changes and this leads to diversity in the receiver currents. As a result, receiver currents will impose an induced voltage on each other. Then, the whole system will suffer from detuned conditions. As a result, both the system efficiency and output power capacity are affected.
- (2) With the different power demands during operation, the equivalent load of the train changes randomly, and may deviate from the designed optimal load value. The random load will greatly influence the system efficiency.

In order to overcome these problems, an analysis of a dual-receiver IPT system is carried out in this paper and a compensation approach to suppress cross coupling influence is proposed. To improve the overall system efficiency, the optimal load reactance is derived according to the relationship between the parasitic resistances and the cross coupling between receivers. Then, a MEPT control scheme is proposed to track the maximum efficiency point.

This paper is organized as follows: Section 2 analyzes the effect of cross coupling between receivers under various operational conditions and an approach to improve overall system efficiency is presented. A MEPT control scheme, in which the inverter searches for the maximum efficiency point and the active rectifiers of the dual receivers regulate the output voltage, is proposed in Section 3. A 2 kW dual-receiver IPT system is set up in Section 4 to verify the performance of MEPT control scheme. Finally, the conclusions of this paper is drawn in Section 5.

2. Analysis on Dual-Coil Receiver IPT System

As illustrated in Figure 2a, the primary side consists of a DC voltage source E , a full-bridge inverter, the transmitter coil L_P with the equivalent series resistance (ESR) R_{LP} and the resonant capacitor C_P . L_P and C_P are supposed to be tuned to be resonant at the switching frequency of the inverter. Each of the two secondary sides consists of the receiver coil L_{S1} (L_{S2}) with the ESR r_{LS1} (r_{LS2}) and an active rectifier. The components of both secondary sides are supposed to be the same. The two active rectifiers are parallel-connected to the DC load R_{dc} . The primary side circuit generates a high frequency current in the transmitter coil, which is loosely coupled with the two receiver coils. The current in the transmitter coil excites an alternative magnetic field and a high frequency voltage is induced in the receiver coil of each receiver. M_{P1} and M_{P2} are the mutual inductances between the transmitter and two receivers. The cross coupling between two receivers is M_{12} . Figure 2b shows the equivalent circuit of the dual-receiver IPT system in which each receiver is connected with one equivalent load resistance seen from the active rectifiers R_1 (R_2). The equivalent load resistance seen from the active rectifiers can be described as follows:

$$\frac{1}{R_1} + \frac{1}{R_2} = \frac{1}{R_{ac}} \quad (1)$$

R_{ac} is defined as the AC equivalent resistance.

2.1. Effect of the Cross Coupling between Two Coils

From the equivalent circuit in Figure 2b, the induced receiver voltages can be expressed as:

$$\begin{cases} \dot{U}_{S1} = -j\omega M_{P1} \dot{I}_P - j\omega M_{12} \dot{I}_2 \\ \dot{U}_{S2} = -j\omega M_{P2} \dot{I}_P - j\omega M_{12} \dot{I}_1 \end{cases} \quad (2)$$

As shown in Equation (2), when $M_{12} = 0$, the induced receiver voltages are independent. When $M_{12} \neq 0$, the amplitude and phase of induced receiver voltages interact with cross coupling

between two receivers, so the cross coupling between receivers could impact the performance of the system and it is necessary to find a way to eliminate the effects of this cross coupling between receivers.

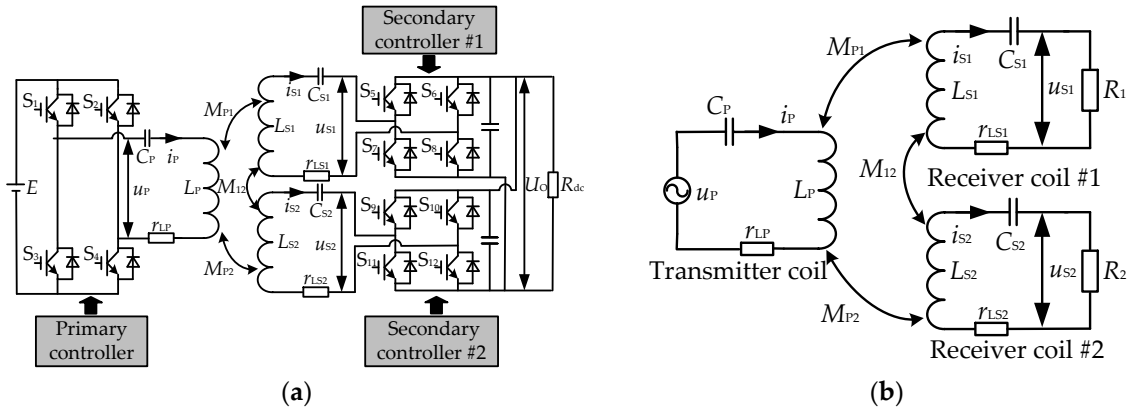


Figure 2. An IPT system based on dual-receiver: (a) The structure of dual-receiver IPT system; (b) The equivalent circuit of dual-receiver IPT system.

2.2. Self-Inductance Compensated Scenario

Based on the assumption that the capacitors in the primary side and the secondary sides fully compensate the self-inductances of the transmitter coil and receiver coils, the ESRs of the coils are r_{LP} , r_{LS1} and r_{LS2} . The receiver coils are identical, so it is assumed that $r_{LS1} = r_{LS2} = r_{LS}$. The relationships between the input voltage \dot{U}_P , the currents \dot{I}_P , \dot{I}_{S1} and \dot{I}_{S2} , can be described according to the Kirchhoff's voltage law as:

$$\begin{bmatrix} \dot{U}_P \\ 0 \\ 0 \end{bmatrix} = \begin{bmatrix} Z_P & j\omega M_{P1} & j\omega M_{P2} \\ j\omega M_{P1} & Z_1 + R_1 & -j\omega M_{12} \\ j\omega M_{P2} & -j\omega M_{12} & Z_2 + R_2 \end{bmatrix} \begin{bmatrix} \dot{I}_P \\ \dot{I}_{S1} \\ \dot{I}_{S2} \end{bmatrix} \quad (3)$$

where:
$$\begin{bmatrix} Z_P \\ Z_1 \\ Z_2 \end{bmatrix} = \begin{bmatrix} j\omega L_P + (j\omega C_P)^{-1} + r_{LP} \\ j\omega L_{S1} + (j\omega C_{S1})^{-1} + r_{LS1} \\ j\omega L_{S2} + (j\omega C_{S2})^{-1} + r_{LS2} \end{bmatrix} = \begin{bmatrix} r_{LP} \\ r_{LS} \\ r_{LS} \end{bmatrix}.$$

By solving Equation (3), the input voltage and receiver currents can be provided by:

$$\begin{bmatrix} \dot{U}_P \\ \dot{I}_{S1} \\ \dot{I}_{S2} \end{bmatrix} = \begin{bmatrix} \frac{\omega^2 M_{P1}^2 (R_2 + r_{LS}) \dot{I}_P + \omega^2 M_{P2}^2 (R_1 + r_{LS}) \dot{I}_P + j2\omega^3 M_{P1} M_{P2} M_{12} \dot{I}_P}{\omega^2 M_{12}^2 + R_1 R_2 + r_{LS}^2 + R_1 r_{LS} + R_2 r_{LS}} + r_P \dot{I}_P \\ \frac{\omega^2 M_{12} M_{P2} \dot{I}_P (R_1 + r_{LS}) - j\omega M_{P1} (R_1 + r_{LS}) (R_2 + r_{LS}) \dot{I}_P}{\omega^2 M_{12}^2 + R_1 R_2 + r_{LS}^2 + R_1 r_{LS} + R_2 r_{LS}} \\ \frac{\omega^2 M_{12} M_{P1} \dot{I}_P (R_2 + r_{LS}) - j\omega M_{P2} (R_1 + r_{LS}) (R_2 + r_{LS}) \dot{I}_P}{\omega^2 M_{12}^2 + R_1 R_2 + r_{LS}^2 + R_1 r_{LS} + R_2 r_{LS}} \end{bmatrix} \quad (4)$$

Assuming the self-inductances of receivers are the same ($L_{S1} = L_{S2} = L_S$), and the mutual inductances between the transmitter and receivers are equal to each other ($M_{P1} = M_{P2} = M_P$), the equivalent load resistances are identical as follows:

$$R_1 = R_2 = 2R_{ac} \quad (5)$$

By substituting Equation (5) into (4), the input voltage and receiver currents can be obtained by:

$$\begin{bmatrix} \dot{U}_P \\ \dot{I}_{S1} \\ \dot{I}_{S2} \end{bmatrix} = \begin{bmatrix} \frac{2\omega^2 M_P^2 \dot{I}_P}{2R_{ac} + r_{LS} - j\omega M_{12}} \\ -\frac{j\omega M_P \dot{I}_P}{2R_{ac} + r_{LS} - j\omega M_{12}} \\ -\frac{j\omega M_P \dot{I}_P}{2R_{ac} + r_{LS} - j\omega M_{12}} \end{bmatrix} \quad (6)$$

According to Equation (6), the primary side and secondary sides are detuned, so the performance of the system is impacted. From Equation (6) with the assumption that $\dot{I}_{S1} = \dot{I}_{S2}$, the output voltage can be described as:

$$\dot{U}_{S1} = \dot{U}_{S2} = -\frac{j\omega M_P \dot{I}_P 2R_{ac}}{2R_{ac} + r_{LS} - j\omega M_{12}} \approx -\frac{j\omega M_P \dot{I}_P 2R_{ac}}{2R_{ac} - j\omega M_{12}} (R_{ac} \gg r_{LS}) \quad (7)$$

When the mutual inductances between the transmitter and two receivers are the same, the cross coupling between receivers will reduce the system output voltage amplitude. The larger the mutual inductance M_{12} is, the more the output voltage will be affected.

The voltage-current gain (the receiver voltage versus transmitter current) is given by:

$$G_{VI} = \frac{|\dot{U}_{S1}|}{|\dot{I}_P|} = \frac{|\dot{I}_{S1} \cdot R_1|}{|\dot{I}_P|} = \frac{2R_{ac}}{\sqrt{(2R_{ac} + r_{LS})^2 + \omega^2 M_{12}^2}} \omega M_P \approx \frac{2R_{ac}}{\sqrt{4R_{ac}^2 + \omega^2 M_{12}^2}} \omega M_P (R_{ac} \gg r_{LS}) \quad (8)$$

In a well-tuned IPT system G_{VI} is not related to the load. Figure 3 shows the relationship between voltage-current gain ratio $\tau = 2R_{ac} / \sqrt{4R_{ac}^2 + \omega^2 M_{12}^2}$ and $\rho = \omega M_{12} / R_{ac}$. The voltage-current gain ratio decreases with the increase of ρ . In other words, the cross coupling between receivers has a serious effect on output voltages under heavy load conditions (small load resistance).

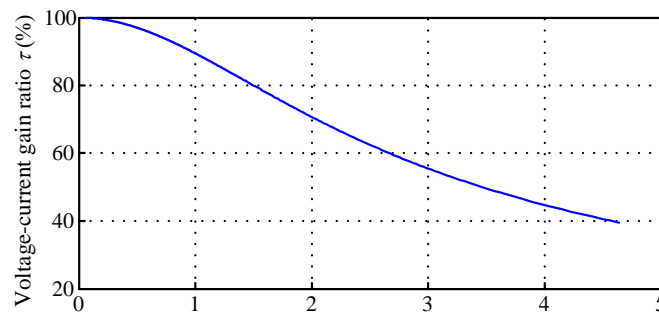


Figure 3. The voltage-current gain ratio curve.

Besides, the output power can be expressed as:

$$P_{out} = \dot{I}_{S1} (\dot{I}_{S1})^* R_1 + \dot{I}_{S2} (\dot{I}_{S2})^* R_2 = \frac{4\omega^2 M_P^2 I_P^2 R_{ac}}{(2R_{ac} + r_{LS})^2 + \omega^2 M_{12}^2} \approx \frac{4\omega^2 M_P^2 I_P^2 R_{ac}}{4R_{ac}^2 + \omega^2 M_{12}^2} (R_{ac} \gg r_{LS}) \quad (9)$$

where * is the conjugate symbol.

Figure 4 shows the relationship between output power ratio $\kappa = 4R_{ac}^2 / (4R_{ac}^2 + \omega^2 M_{12}^2)$ and ρ . According to Figure 4, the output power ratio decreases with the increase of ρ . When $\rho = 1$, the output power is equal to 80% of a well-tuned one.

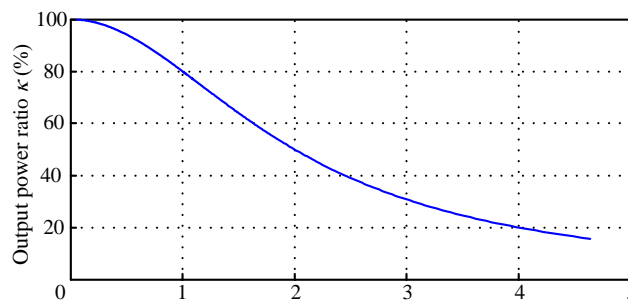


Figure 4. The output power ratio curve.

From Equations (8) and (9), the cross coupling between receivers reduces both the output power and the voltage-current gain (the receiver voltage versus transmitter current). The cross coupling between receivers would seriously affect IPT system in heavy load situations. Therefore, it is necessary to find a way to suppress the adverse effects of cross coupling between receivers.

2.3. Cross Coupling Compensated Scenario

In order to compensate the cross coupling between the two receivers, additional reactance is applied in the secondary sides to overcome the drawbacks caused by the cross coupling between receivers as shown in following equation:

$$\begin{bmatrix} \dot{U}_P \\ 0 \\ 0 \end{bmatrix} = \begin{bmatrix} Z_P & j\omega M_P & j\omega M_P \\ j\omega M_P & Z_1 + R_1 & -j\omega M_{12} \\ j\omega M_P & -j\omega M_{12} & Z_2 + R_2 \end{bmatrix} \begin{bmatrix} \dot{I}_P \\ \dot{I}_{S1} \\ \dot{I}_{S2} \end{bmatrix} \quad (10)$$

where:
$$\begin{bmatrix} Z_P \\ Z_1 \\ Z_2 \end{bmatrix} = \begin{bmatrix} j\omega L_P + (j\omega C_P)^{-1} + r_{LP} \\ j\omega L_{S1} + (j\omega C_{S1})^{-1} + r_{LS1} \\ j\omega L_{S2} + (j\omega C_{S2})^{-1} + r_{LS2} \end{bmatrix} = \begin{bmatrix} r_{LP} \\ jX_{S1} + r_{LS} \\ jX_{S2} + r_{LS} \end{bmatrix}$$

X_{S1} and X_{S2} are the additional reactances supposed to be added in the secondary sides. By solving Equation (10), the input voltage and receiver currents can be obtained by:

$$\begin{bmatrix} \dot{U}_P \\ \dot{I}_{S1} \\ \dot{I}_{S2} \end{bmatrix} = \begin{bmatrix} \frac{2\omega^2 \dot{I}_P M_P^2 (R + r_{LS} - jX + j\omega M_{12})}{(X_S - \omega M_{12})^2 + (R + r_{LS})^2} + r_{LP} \dot{I}_P \\ -\frac{\omega M_P \dot{I}_P (X_S - \omega M_{12}) + j\omega M_P \dot{I}_P (R + r_{LS})}{(X_S - \omega M_{12})^2 + (R + r_{LS})^2} \\ -\frac{\omega M_P \dot{I}_P (X_S - \omega M_{12}) + j\omega M_P \dot{I}_P (R + r_{LS})}{(X_S - \omega M_{12})^2 + (R + r_{LS})^2} \end{bmatrix} \quad (11)$$

According to Equation (11), the apparent power transferred from the transmitter to the secondary sides can be described as follows:

$$S = \dot{U}_S (\dot{I}_{S1}^* + \dot{I}_{S2}^*) = -j\omega M_P \dot{I}_P (\dot{I}_{S1}^* + \dot{I}_{S2}^*) = \frac{2\omega^2 \dot{I}_P^2 M_P^2 (R + r_{LS} + jX_S - j\omega M_{12})}{\omega^2 M_{12}^2 + X_S^2 - 2\omega M_{12} X_S + (R + r_{LS})^2} \quad (12)$$

Let the imaginary part of Equation (12) be zero:

$$X_S - \omega M_{12} = 0 \quad (13)$$

Then, X_S can be expressed as:

$$X_S = \omega M_{12} \quad (14)$$

By substituting Equation (14) into Z_1 and Z_2 , the compensated capacitor is derived as:

$$C_S = \frac{1}{\omega^2 (L_S - M_{12})} \quad (15)$$

Then Equation (11) can be simplified as:

$$\begin{bmatrix} \dot{U}_P \\ \dot{I}_{S1} \\ \dot{I}_{S2} \end{bmatrix} = \begin{bmatrix} \frac{2\omega^2 \dot{I}_P M_P^2}{2R_{ac} + r_{LS}} + r_{LP} \dot{I}_P \\ -\frac{j\omega M_P \dot{I}_P}{2R_{ac} + r_{LS}} \\ -\frac{j\omega M_P \dot{I}_P}{2R_{ac} + r_{LS}} \end{bmatrix} \quad (16)$$

From Equation (16), the output voltage can be described as:

$$\dot{U}_{S1} = \dot{U}_{S2} = -\frac{j\omega M_P \dot{I}_P 2R_{ac}}{2R_{ac} + r_{LS}} \approx -j\omega M_P \dot{I}_P (R_{ac} \gg r_{LS}) \quad (17)$$

From Equation (17), when the mutual inductances between the transmitter and two receivers are the same, additional capacitors could be added to tune the IPT system.

The voltage-current gain (the receiver voltage versus transmitter current):

$$G_{VI} = \frac{|\dot{U}_{S1}|}{|\dot{I}_P|} = \frac{|\dot{I}_{S1} \cdot R_1|}{|\dot{I}_P|} = \frac{2R_{ac}}{2R_{ac} + r_{LS}} \omega M_P \approx \omega M_P (R_{ac} \gg r_{LS}) \quad (18)$$

The output power is attained by:

$$P_{out} = \dot{I}_{S1} (\dot{I}_{S1})^* R_1 + \dot{I}_{S2} (\dot{I}_{S2})^* R_2 = \frac{2\omega^2 \dot{I}_P M_P^2}{2R_{ac} + r_{LS}} \approx \frac{\omega^2 \dot{I}_P M_P^2}{R_{ac}} (R_{ac} \gg r_{LS}) \quad (19)$$

The adverse influence of the mutual inductance between receivers can be eliminated by additional capacitors added to the secondary side. Not only the voltage-current gain (the receiver voltage versus transmitter current) can be improved, but also more power can be transferred from the transmitter to the receivers.

2.4. Different Mutual Inductance Scenario

The mutual inductances between the transmitter and receivers would change as the receivers move along the transmitter track. Letting $M_{P1} = \lambda M_{P2}$ and substituting Equation (15) into (10), Equation (10) can be simplified as follows:

$$\begin{bmatrix} \dot{U}_P \\ 0 \\ 0 \end{bmatrix} = \begin{bmatrix} Z_P & j\omega \lambda M_{P2} & j\omega M_{P2} \\ j\omega M_{P1} & j\omega M_{12} + R_1 + r_{LS} & -j\omega M_{12} \\ j\omega M_{P2} & -j\omega M_{12} & j\omega M_{12} + R_2 + r_{LS} \end{bmatrix} \begin{bmatrix} \dot{I}_P \\ \dot{I}_{S1} \\ \dot{I}_{S2} \end{bmatrix} \quad (20)$$

By solving Equation (20), the input voltage and receiver currents can be provided by:

$$\begin{cases} \dot{U}_P = \frac{\lambda \omega M_{P2} B_1 + \omega M_{P2} B_2 + j\lambda \omega M_{P2} A_1 + j\omega M_{P2} A_2}{\omega^2 M_{12}^2 (R_1 + r_{LS})^2 + 2\omega^2 M_{12}^2 (R_1 + r_{LS})(R_2 + r_{LS}) + \omega^2 M_{12}^2 (R_2 + r_{LS})^2 + (R_1 + r_{LS})^2 (R_2 + r_{LS})^2} \\ \dot{I}_{S1} = -\frac{A_1 + jB_1}{\omega^2 M_{12}^2 (R_1 + r_{LS})^2 + 2\omega^2 M_{12}^2 (R_1 + r_{LS})(R_2 + r_{LS}) + \omega^2 M_{12}^2 (R_2 + r_{LS})^2 + (R_1 + r_{LS})^2 (R_2 + r_{LS})^2} \\ \dot{I}_{S2} = -\frac{A_2 + jB_2}{\omega^2 M_{12}^2 (R_1 + r_{LS})^2 + 2\omega^2 M_{12}^2 (R_1 + r_{LS})(R_2 + r_{LS}) + \omega^2 M_{12}^2 (R_2 + r_{LS})^2 + (R_1 + r_{LS})^2 (R_2 + r_{LS})^2} \end{cases} \quad (21)$$

$$\text{where: } \begin{bmatrix} A_1 \\ A_2 \\ B_1 \\ B_2 \end{bmatrix} = \begin{bmatrix} \omega^2 M_{12} M_{P2} I_P (R_2 + r_{LS}) [\lambda (R_2 + r_{LS}) - (R_1 + r_{LS})] \\ \omega^2 M_{12} M_{P2} I_P (R_1 + r_{LS}) [(R_1 + r_{LS}) - \lambda (R_2 + r_{LS})] \\ \omega^3 M_{12}^2 I_P M_{P2} (\lambda + 1) (R_1 + R_2 + 2r_{LS}) + \lambda \omega M_{P2} I_P (R_1 + r_{LS}) (R_2 + r_{LS})^2 \\ \omega^3 M_{12}^2 I_P M_{P2} (\lambda + 1) (R_1 + R_2 + 2r_{LS}) + \lambda \omega M_{P2} I_P (R_1 + r_{LS})^2 (R_2 + r_{LS}) \end{bmatrix}$$

According to Equation (21), when the mutual inductances between the transmitter and two receivers are different, the amplitude and phase of receiver currents are different from each other. Reactive power is transferred amongst the transmitter and receivers. The additional capacitor compensation only works under the condition that two receiver currents are identical.

With these relationships, the apparent output power is given by:

$$\begin{aligned} S &= -j\omega M_{P1} \dot{I}_P \dot{I}_{S1}^* - j\omega M_{P2} \dot{I}_P \dot{I}_{S2}^* \\ &= \frac{\omega \dot{I}_P M_{P2} (\lambda B_1 + B_2) - j\omega \dot{I}_P M_{P2} (\lambda A_1 + A_2)}{\omega^2 M_{12}^2 (R_1 + r_{LS})^2 + 2\omega^2 M_{12}^2 (R_1 + r_{LS})(R_2 + r_{LS}) + \omega^2 M_{12}^2 (R_2 + r_{LS})^2 + (R_1 + r_{LS})^2 (R_2 + r_{LS})^2} \end{aligned} \quad (22)$$

Let the imaginary component of Equation (22) be zero:

$$\omega \dot{I}_P M_{P2} (\lambda A_1 + A_2) = -\omega^3 M_{12} M_{P2}^2 I_P^2 [(R_1 + r_{LS}) - \lambda(R_2 + r_{LS})]^2 = 0 \quad (23)$$

$R_1 \gg r_{LS}$ and $R_2 \gg r_{LS}$, then R_1 can be solved as:

$$R_1 \approx \lambda R_2 \quad (24)$$

From Equations (1) and (24), R_1 and R_2 can be expressed as:

$$\begin{bmatrix} R_2 \\ R_1 \end{bmatrix} = \begin{bmatrix} \lambda^{-1}(\lambda + 1)R_{ac} \\ (\lambda + 1)R_{ac} \end{bmatrix} \quad (25)$$

By substituting Equation (25) into (21), we have:

$$\begin{cases} \dot{U}_P = \frac{\omega^2 M_{P2} \dot{I}_P (M_{P1} + M_{P2})}{R_2} \\ \dot{I}_{S1} = \frac{-j\omega M_{P2} \dot{I}_P}{\lambda^{-1}(\lambda + 1)R_{ac}} \\ \dot{I}_{S2} = \frac{-j\omega M_{P2} \dot{I}_P}{\lambda^{-1}(\lambda + 1)R_{ac}} \end{cases} \quad (26)$$

Hence, in order to tune the system with different mutual inductances M_{P1} and M_{P2} , the receiver currents should be controlled to be the same as shown in Equation (26). When Equation (26) is met, the output voltage and the output power of two receivers can be described as:

$$\begin{cases} \dot{U}_{S1} = \lambda \dot{U}_{S2} \\ P_1 = \lambda P_2 \end{cases} \quad (27)$$

It is clear that the difference of the two mutual inductances between the transmitter and the receivers changes the resonance characteristics of the system. Only when receiver currents are identical, the cross coupling between receivers can be compensated by a capacitor. Then the whole system is under resonant conditions. Not only under light load conditions, but also under heavy load conditions, the whole system can be operated under resonant conditions.

2.5. Adjust the Receiver Current

The RMS value of the first order harmonic of one active rectifier's input voltage can be expressed as [21]:

$$U_{rec} = \frac{2\sqrt{2}}{\pi} U_O \sin\left(\frac{\alpha}{2}\right) \quad (28)$$

where α is the pulse width of the active rectifier.

As shown in Figure 5, the output DC current can be described as:

$$I_O = \frac{1}{\pi} \int_{\frac{\pi}{2} - \frac{\alpha}{2}}^{\frac{\pi}{2} + \frac{\alpha}{2}} \sqrt{2} I_S \sin(\omega t) dt = \frac{2\sqrt{2}}{\pi} I_S \sin\left(\frac{\alpha}{2}\right) \quad (29)$$

According to Equations (28) and (29), the equivalent input resistance of each active rectifier can be described as:

$$R_{aceq} = \frac{U_{rec}}{I_S} = \frac{8}{\pi^2} \frac{U_O}{I_O} \sin^2\left(\frac{\alpha}{2}\right) = \frac{8}{\pi^2} R_{dc} \sin^2\left(\frac{\alpha}{2}\right) \quad (30)$$

From Equation (30), the resistance seen from the active rectifiers changes according to the pulse widths of active rectifiers. When the mutual inductances between the transmitter and receivers are different, active receiver currents are different from each other. According to Equations (26) and (30), the reduction of the pulse widths of active rectifiers could decrease its equivalent resistance and

increases its current. Therefore, by adjusting the pulse width of active rectifier, active receiver currents could be regulated to be identical and a tuned IPT system is obtained.

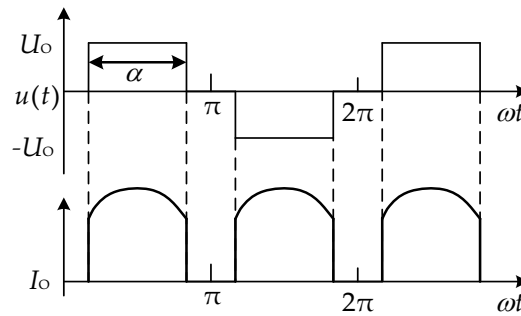


Figure 5. Waveforms of the input voltage and output current of one active rectifier.

2.6. Maximum Efficiency Point

In order to analyze the maximum efficiency point of the system, ESRs of the coils (r_{LP} , r_{LS1} and r_{LS2}) are taken into account. When receiver currents are the same at all the same. Letting $\dot{I}_{S1} = \dot{I}_{S2} = \dot{I}_S$, $r_{LS1} = r_{LS2} = r_{LS}$ and substituting Equation (24) into (20), Equation (20) can be simplified as follows:

$$\begin{bmatrix} \dot{U}_P \\ 0 \\ 0 \end{bmatrix} = \begin{bmatrix} Z_P & j\omega\lambda M_{P2} & j\omega M_{P2} \\ j\omega\lambda M_{P2} & \lambda R_2 + r_{LS} + j\omega M_{12} & -j\omega M_{12} \\ j\omega M_{P2} & -j\omega M_{12} & R_2 + r_{LS} + j\omega M_{12} \end{bmatrix} \begin{bmatrix} \dot{I}_P \\ \dot{I}_S \\ \dot{I}_S \end{bmatrix} \quad (31)$$

The input and output currents can be solved as:

$$\begin{bmatrix} \dot{I}_P \\ \dot{I}_S \end{bmatrix} = \begin{bmatrix} \frac{\dot{U}_P(R_2 + r_{LS})}{(1 + \lambda)\omega^2 M_{P2}^2 + R_2 r_{LP} + r_{LP} r_{LS}} \\ \frac{j\omega \dot{U}_P M_{P2}}{(1 + \lambda)\omega^2 M_{P2}^2 + R_2 r_{LP} + r_{LP} r_{LS}} \end{bmatrix} \quad (32)$$

The output and input power are obtained by:

$$\begin{bmatrix} P_1 \\ P_2 \end{bmatrix} = \begin{bmatrix} \frac{\omega^2 \dot{U}_P^2 M_{P2}^2 \lambda R_2}{((1 + \lambda)\omega^2 M_{P2}^2 + r_{LP} R_2 + r_{LP} r_{LS})^2} \\ \frac{\omega^2 \dot{U}_P^2 M_{P2}^2 R_2}{((1 + \lambda)\omega^2 M_{P2}^2 + r_{LP} R_2 + r_{LP} r_{LS})^2} \end{bmatrix} \quad (33)$$

$$P_{in} = \text{Re}(\dot{U}_P \dot{I}_P^*) = \frac{\dot{U}_P^2 (r_{LS} + R_2)}{(1 + \lambda)\omega^2 M_{P2}^2 + R_2 r_{LP} + r_{LP} r_{LS}} \quad (34)$$

Then the efficiency of the system can be derived by:

$$\eta = \frac{P_1 + P_2}{P_{in}} = \frac{\omega^2 M_{P2}^2 R_2 (1 + \lambda)}{(R_2 + r_{LS})((1 + \lambda)\omega^2 M_{P2}^2 + R_2 r_{LP} + r_{LP} r_{LS})} \quad (35)$$

By substituting Equation (25) into Equation (35), the system efficiency can be expressed as:

$$\eta = \frac{P_1 + P_2}{P_{in}} = \frac{\lambda(\lambda + 1)^2 \omega^2 M_{P2}^2 R_{ac}}{(\lambda R_{ac} + \lambda r_{LS} + R_{ac})(\lambda \omega^2 M_{P2}^2 + \lambda^2 \omega^2 M_{P2}^2 + \lambda r_{LP} R_{ac} + \lambda r_{LP} r_{LS} + r_{LP} R_{ac})} \quad (36)$$

According to Equation (36), the system efficiency is related to the load resistance value. The relationship between the system efficiency and the load resistance value is plotted in Figure 6. It is clear that a maximum efficiency point exists with the variation of the load. The resistance value

corresponding to the maximum efficiency point can be solved by setting the derivative of the system efficiency to be zero as follows:

$$\frac{d\eta}{dR_{ac}} = 0 \tag{37}$$

Then the optimum load can be solved as:

$$R_{op} = \frac{\sqrt{r_{LS}} \sqrt{\omega^2 M_{P2}^2 + \lambda \omega^2 M_{P2}^2 + r_{LP} r_{LS}}}{(1 + \lambda) \sqrt{r_{LP}}} \tag{38}$$

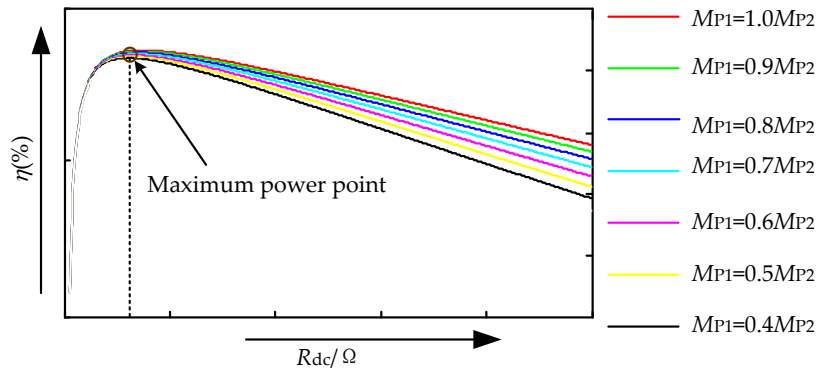


Figure 6. The efficiency of the IPT system versus the load.

3. Control Method

In multiple-receiver IPT applications for railway transportation, the mutual inductances between the transmitter coil and different receiver coils vary as the trains move along the track. As discussed in Section 2, different mutual inductances lead to different receiver currents and cause detuning of the IPT system. Therefore, a receiver current balance control is necessary to suppress the effect of the variation of the mutual inductances. Meanwhile, the output voltage needs to be regulated under all situations. Besides, the load may change during dynamic charging and the system efficiency may decrease with the variation of the load. Therefore, a MEPT control is needed for the efficiency optimization during dynamic charging operation. In general, three control goals (regulating the output voltage, regulating active rectifier currents and improving the overall system efficiency) are set up for the MEPT. Based on the theoretical analysis in Section 2, the control block of the proposed method is shown in Figure 7. Three control loops are illustrated in the control block, respectively.

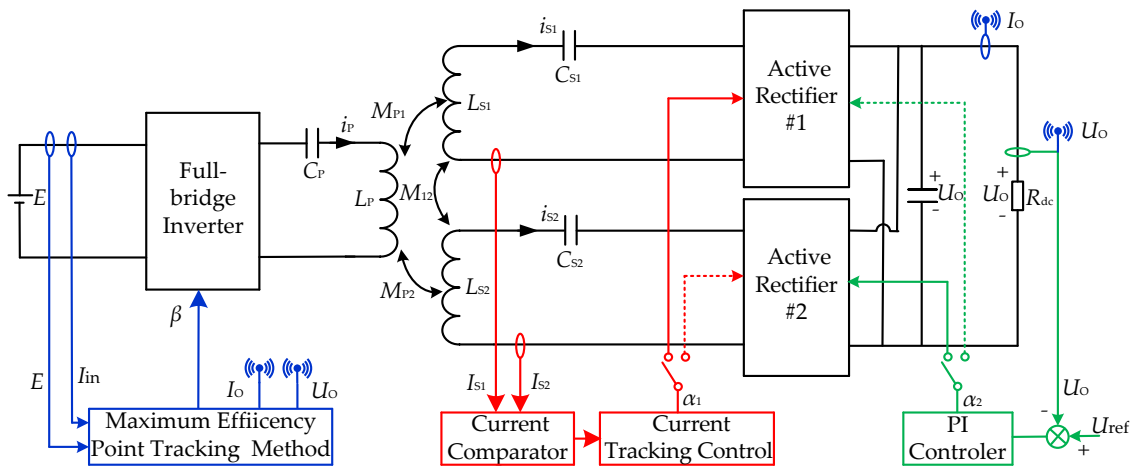


Figure 7. Control scheme of the proposed method.

3.1. Active Rectifier Current Control Loop

The current tracking control block with one current comparator is applied in the secondary sides to balance the two active rectifier currents against the variation of the two mutual inductances M_{P1} and M_{P2} . The detailed control flowchart is shown in Figure 8. D_{S1} and D_{S2} are the pulse widths of active rectifiers on the secondary sides. The active rectifier with smaller pulse width regulates its current to be the same as another one with high induced voltage (larger pulse width). If the pulse width of active rectifier #1 is equal to that of active rectifier #2, the larger current of active rectifier is treated as the reference and a PI controller is adapted to decrease the pulse width of active rectifier with smaller current to increase its current. If the pulse width of active rectifier #1 is larger, current of active rectifier #1 is treated as the reference current, and a PI controller is adopted to decrease (increase) the pulse width of active rectifier #2 to increase (decrease) its current until it hits the same value as that of active rectifier #1, and vice versa.

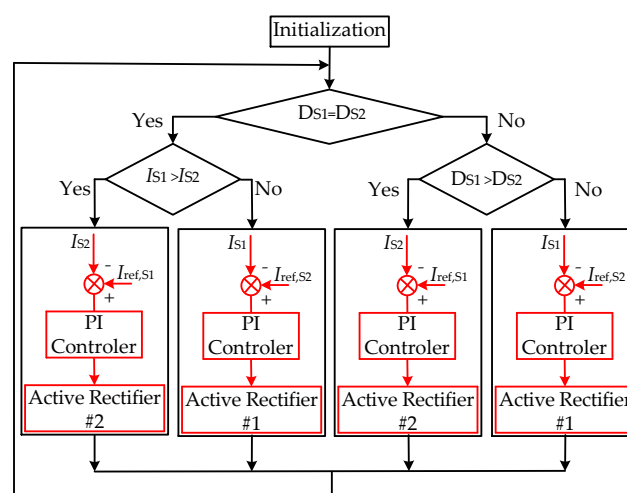


Figure 8. Flow chart of the current tracking control.

3.2. Output Voltage Control Loop

A PI controller is adopted to regulate the system output voltage by adjusting the larger pulse width of active rectifier.

3.3. Perturbation and Observation Control Loop

The MEPT control is carried out by the inverter in the primary side. A perturbation and observation method is adopted to search for the maximum efficiency point as shown in Figure 9. U_O , I_O , E , and I_{in} are the measured load voltage, load current, power supply voltage and current, respectively. The $\eta(n)$ and $\eta(n - 1)$ indicate new data and old data of system overall efficiency. The system overall efficiency η is calculated the measurements of the input and output power. D_P is the conduction angle of the inverter in the primary side. A perturbation ΔD_P is applied in a step-by-step manner in order to search the maximum efficiency point. For each perturbation, the change of system efficiency $\Delta\eta$ ($\Delta\eta = \eta(n) - \eta(n - 1)$) is calculated. If $\Delta\eta$ is positive, the perturbation direction stays the same and the system gradually approaches the maximum efficiency point. On the contrary, the perturbation direction needs to be inverted to search the maximum efficiency point.

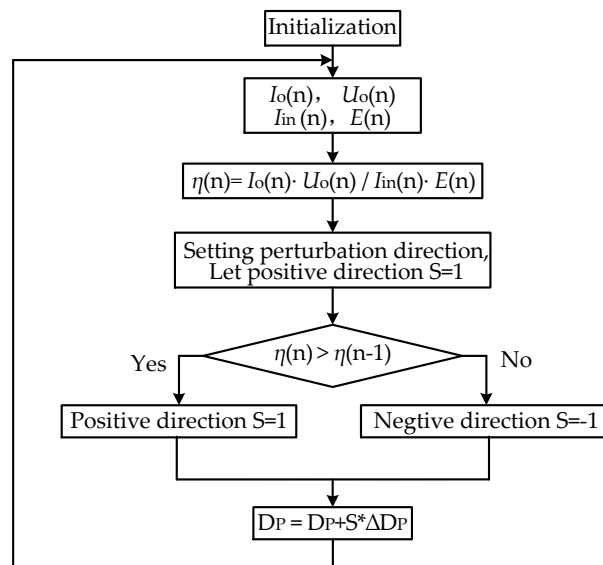


Figure 9. Flow chart of the MEPT control.

4. Experimental Verification

4.1. Experimental Parameters

In order to validate the proposed control method, a prototype multiple-receiver IPT system based on a series-series compensation network was built as shown in Figure 10. A power analyzer, (PW6001, HIOKI, Nagano, Japan) is used for the power and efficiency measurement. An electronic load (IT8518B, ITECH, Immokalee, FL, USA) is used as a controllable load to test the performance of the proposed algorithm. The prototype consists of a DC power supply, a transmitter, two identical receivers and a DC electronic load. The transmitter and receiver coils are wound by Litz wires. All the coils are tuned to resonate at 20 kHz with series capacitors considering the cross coupling between the receiver coils. The parameters of the experimental setup can be found in Table 1. The input DC voltage and the output DC voltage are set to 150 V and 80 V respectively. The rated transmission power of system is designed to be 2 kW. The transmitter coil and receiver coils with ferrites are shown in Figure 11. Turn number of the transmitter coil is 12 and turn number of the receiver coils are both equal to 15.5. Aluminum plates are adopted to shield the unwanted magnetic field on the secondary sides.

Table 1. System Parameters.

Parameters	Value
The input voltage of inverter (E/V)	150
Operating frequency (f/kHz)	20
Inductance of transmitter coil ($L_P/\mu H$)	465.17
Compensating capacitor of transmitter coil (C_P/nF)	136.13
Inductance of receiver coil 1 ($L_{S1}/\mu H$)	222.23
Inductance of receiver coil 2 ($L_{S2}/\mu H$)	222.54
Crossing coupling between dual-coil receiver ($M_{12}/\mu H$)	21.15
Compensating capacitor of receiver coil 1 ($C_{S1}/\mu F$)	315.02
Compensating capacitor of receiver coil 2 ($C_{S2}/\mu F$)	315.03
DC load (R_{dc}/Ω)	3.5–10

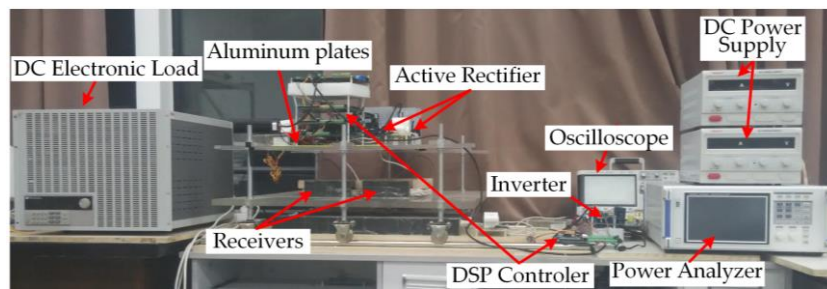


Figure 10. Experimental setup.



Figure 11. Setup of the transmitter coil and the receiver coils.

In the experimental setup, receivers mounted in a trolley that can be moved freely along the track to simulate the dynamic charging scenarios in practical IPT applications. The mutual inductances between the transmitter coil and the receiver coils are a function of the relative positions between the track and the trolley. The track and the moving trolley's diagrammatic sketch is shown in Figure 12. δ indicates the relative position shift between the center of the transmitter track and the receivers.

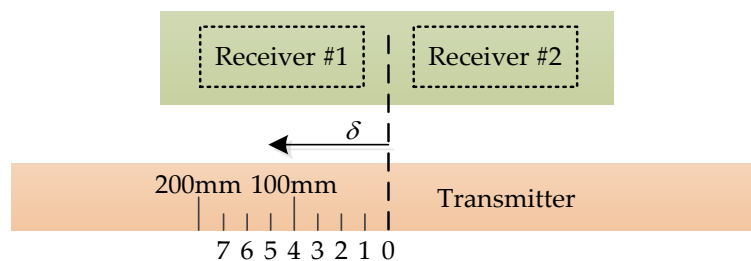


Figure 12. Diagrammatic sketch of the track and trolley.

4.2. Experimental Results

In order to verify the feasibility of the current tracking control method, the position of the receivers is changed in various test cases to simulate practical operation conditions. Figure 13 shows the steady waveforms of the input voltages of the active rectifiers and the receiver currents when the receivers are in alignment with the transmitter track where M_{P1} is equal to M_{P2} . The pulse widths of the two active rectifiers are the same while i_{S1} is nearly identical to i_{S2} . When the position shift $\delta = 100$ mm between the center of the transmitter track and the receivers, i_{S1} and i_{S2} differs slightly, as shown in Figure 14a, due to the small difference between M_{P1} and M_{P2} . By applying the proposed method which adjusts the pulse widths of the two active rectifiers, i_{S1} and i_{S2} are controlled to be the as shown in Figure 14b. When $\delta = 175$ mm, the difference between M_{P1} and M_{P2} becomes larger which leads to the apparent unbalance of the two receiver currents and the phase difference of the input voltages of the two active rectifiers as shown in Figure 15a. The RMS value of i_{S1} and i_{S2} are 7.2 A and 1.6 A respectively and the corresponding difference is nearly 5.6 A. Similarly, in Figure 15b, the pulse widths of the two active

rectifiers are adjusted to regulate i_{s1} and i_{s2} to be the same with the proposed method. When the output DC voltage is set to 80 V and the load is set to 10Ω in Figures 13–15, the output power of active rectifiers can be obtained. According to the data in Table 2, the unbalance of the active rectifiers' output power has gradually increased without the current control. The current control could significantly improve the unbalance of the active rectifiers' output power.

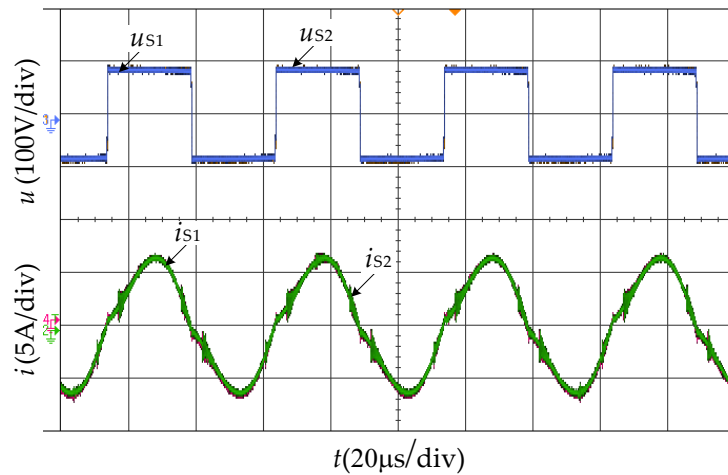


Figure 13. Input voltage and current waveforms of the receivers when the load is 10Ω and δ equals 0.

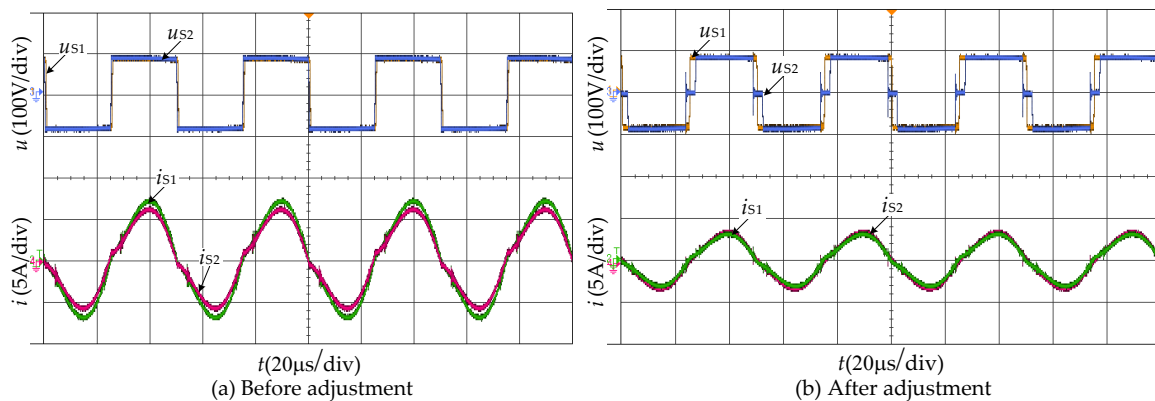


Figure 14. Input voltage and current waveforms of the receivers when the load is 10Ω and δ equals 100 mm.

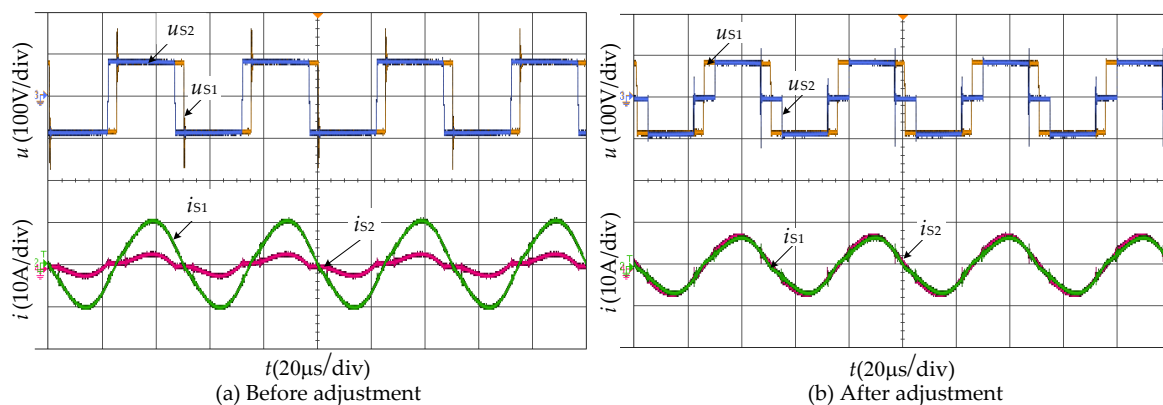


Figure 15. Input voltage and current waveforms of the receivers when the load is 10Ω and δ equals 175 mm.

Table 2. The output power of receivers before and after the current control applied.

Position/(mm)	Mutual Inductance		Before Adjustment		After Adjustment	
	$M_{P1}/\mu\text{H}$	$M_{P2}/\mu\text{H}$	Output Power of Rectifier #1/(W)	Output Power of Rectifier #2/(W)	Output Power of Rectifier #1/(W)	Output Power of Rectifier #2/(W)
$\delta = 0$	43.33	43.32	336	337	336	337
$\delta = 100$	43.59	42.92	365	305	343	319
$\delta = 175$	44.12	38.82	542	123	347	315

For the purpose of evaluating the performance on efficiency improvement of the proposed algorithm, another two algorithms are employed for comparison with the algorithm presented here under various conditions:

- (1) Controlled inverter and uncontrolled active rectifier (CIUR) mode. The pulse widths of the MOSFETs of the active rectifier is set to 180 degree (passive-rectifier) and the conduction angle of the inverter is controlled to regulate the output voltage of DC load bus.
- (2) Uncontrolled inverter and controlled active rectifier (UICR) mode. The conduction angle of the inverter is set to 180 degree and the MOSFETs of the active rectifier are controlled to regulate the output voltage of DC load bus and regulate the receiver currents to be the same.

The system efficiency curves with different control methods are shown in Figure 16 against various positions under constant load (9 Ω). The voltage of the DC load bus is regulated as 80 V in all experiments. Due to the decrease of the mutual inductances between the transmitter coil and the receiver coils, all the efficiency curves with different algorithms go down as the trolley moves away from the center of the track. It is clear that the system efficiency with the proposed algorithm is much higher than that of other two algorithms at all positions, which coincides with the analysis in Section 2. The system efficiency with proposed method can be improved by about 5.5% compared with UICR mode and by about 2.5% compared with CIUR mode.

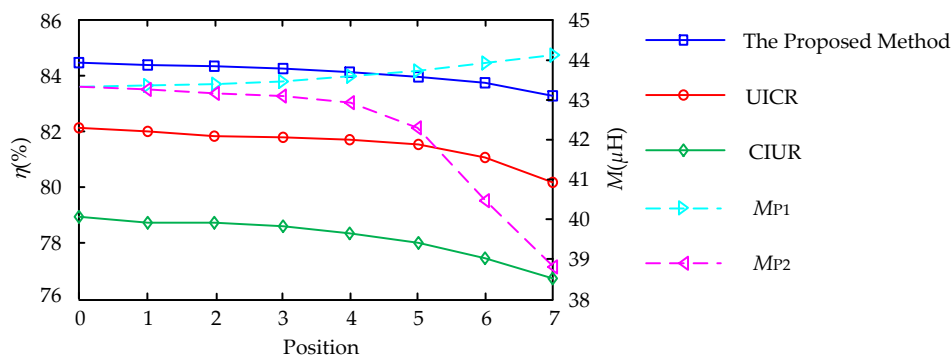
**Figure 16.** The efficiency of IPT system at various positions under constant load.

Figure 17 shows the system efficiency curves with different control methods under various loads when δ equals 150 mm. Under heavy load condition, the three algorithms have nearly the same efficiency as the conduction angle of the inverter and the active rectifier are equal to 180 degrees, so the efficiency of the three methods is the same (90.6%). When the equivalent load resistance goes from 3.5 Ω to 6 Ω (the optimal resistance), the performance of the CIUR method decreases dramatically due to the lack of the control of the two parallel active rectifier currents. When the equivalent resistance is larger than 6 Ω , the efficiency of the proposed method is higher than that of UICR, as the proposed method can control the optimized resistance via an efficiency control loop by lowering the equivalent resistance.

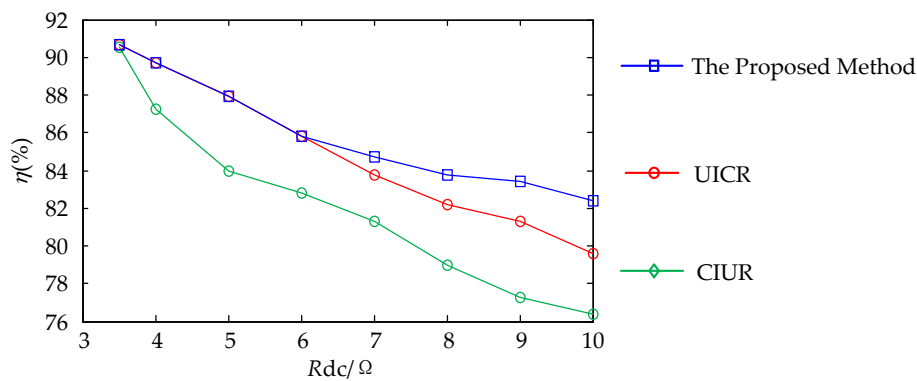


Figure 17. The efficiency of the IPT system when changing the DC load when δ equals 150 mm.

5. Conclusions

In this study, a method to track the maximum efficiency point for dynamic wireless power supply systems against the variation of the load and the mutual inductances between the transmitter and receivers is proposed. According to the theoretical analysis, the cross coupling between receivers decreases the system efficiency and the output power. Extra compensation should be considered to compensate this cross coupling between receivers. Meanwhile, the variation of mutual inductance between the transmitter and the receivers causes detuning of the system. By controlling the receiver currents to be the same, the effect of mutual inductances can be suppressed. In the control scheme, the smaller pulse widths of active rectifiers are adopted to regulate the receiver currents to be the same. The larger pulse widths of active rectifiers is used to regulate the system output voltage. The inverter on the primary side is utilized to improve the system efficiency based on the perturbation and observation approach. The proposed method has been validated by experiments in a 2 kW prototype. The current tracking control is able to regulate the receiver current to be the same when the receivers move along the transmitter track. The system efficiency reaches 90.6% at rated power. Furthermore, the system efficiency with the proposed method is improved by 5.8% under light load compared with the traditional constant output voltage control method. The improvement of the system performance is at the cost of being more complicated than the passive-rectifier approach. The proposed approach needs five measurements (DC output voltage, currents of receivers, DC input voltage and DC input current) and three controllers (two PI controllers and a perturbation and observation controller), while the typical passive-rectifier approach only needs the DC output voltage and one PI controller.

Acknowledgments: This work was supported by the National Science Foundation for Distinguished Young Scholars of China under Grant No. 51525702, the National Natural Science Foundation of China under Grant No. 51677155, the Independent Research Subject of the State Key Laboratory of Traction Power under Grant No. 2016TPL_T11.

Author Contributions: Ruikun Mai proposed the idea and analyzed the data this paper; Linsen Ma designed and performed the experiments; Yeran Liu, Guangzhong Cao and Zhengyou He analyzed the data. All authors contributed to the writing of the manuscript, and have read and approved the final manuscript.

Conflicts of Interest: The authors declare no conflict of interest.

References

1. Covic, G.A.; Boys, J.T. Inductive Power Transfer. *IEEE Proc.* **2013**, *101*, 1276–1289. [[CrossRef](#)]
2. Boys, J.T.; Covic, G.A.; Green, A.W. Stability and control of inductively coupled power transfer systems. *IEE Proc. Electr. Power Appl.* **2000**, *147*, 37–43. [[CrossRef](#)]
3. Hui, S.; Ho, W.W. A new generation of universal contactless battery charging platform for portable consumer electronic equipment. *IEEE Trans. Power Electron.* **2005**, *20*, 620–627. [[CrossRef](#)]
4. Hu, A.P.; Hussmann, S. Improved power flow control for contactless moving sensor applications. *IEEE Power Electron. Lett.* **2004**, *2*, 135–138. [[CrossRef](#)]

5. Choi, S.Y.; Gu, B.W.; Jeong, S.Y.; Rim, C.T. Advances in Wireless Power Transfer Systems for Roadway-Powered Electric Vehicles. *IEEE J. Emerg. Sel. Top. Power Electron.* **2015**, *3*, 18–36. [[CrossRef](#)]
6. Kim, J.H.; Lee, B.-S.; Lee, J.-H.; Lee, S.-H.; Park, C.-B.; Jung, S.-M.; Lee, S.-G.; Yi, K.-P.; Baek, J. Development of 1-MW Inductive Power Transfer System for a High-Speed Train. *IEEE Trans. Ind. Electron.* **2015**, *62*, 6242–6250. [[CrossRef](#)]
7. Huh, J.; Lee, S.W.; Lee, W.Y.; Cho, G.H.; Rim, C.T. Narrow-Width Inductive Power Transfer System for Online Electrical Vehicles. *IEEE Trans. Power Electron.* **2011**, *26*, 3666–3679. [[CrossRef](#)]
8. Woronowicz, K.; Safaee, A.; Dickson, T. A general approach to tuning of a dual secondary winding transformer for wireless power transfer. In Proceedings of the 2014 IEEE International Electric Vehicle Conference (IEVC), Florence, Italy, 17–19 December 2014.
9. Monti, G.; Che, W.; Wang, Q.; Dionigi, M.; Mongiardo, M.; Perfetti, R.; Chang, Y. Wireless power transfer between one transmitter and two receivers: Optimal analytical solution. *Wirel. Power Transf.* **2016**, *3*, 63–73. [[CrossRef](#)]
10. Fu, M.; Zhang, T.; Ma, C.; Zhu, X. Efficiency and optimal loads analysis for multiple-receiver wireless power transfer systems. *IEEE Trans. Microw. Theory Tech.* **2015**, *63*, 801–812. [[CrossRef](#)]
11. Ahn, D.; Hong, S. Effect of coupling between multiple transmitters or multiple receivers on wireless power transfer. *IEEE Trans. Ind. Electron.* **2013**, *60*, 2602–2613. [[CrossRef](#)]
12. Fu, M.; Zhang, T.; Zhu, X.; Luk, P.C.-K.; Ma, C. Compensation of Cross Coupling in Multiple-Receiver Wireless Power Transfer Systems. *IEEE Trans. Ind. Inform.* **2016**, *12*, 474–482. [[CrossRef](#)]
13. Kim, J.; Son, H.-C.; Kim, D.-H.; Park, Y.-J. Impedance matching considering cross coupling for wireless power transfer to multiple receivers. In Proceedings of the 2013 IEEE Wireless Power Transfer (WPT), Perugia, Italy, 15–16 May 2013; pp. 226–229.
14. Ean, K.K.; Chuan, B.T.; Imura, T.; Hori, Y. Impedance matching and power division algorithm considering cross coupling for wireless power transfer via magnetic resonance. In Proceedings of the 2012 IEEE 34th International Telecommunications Energy Conference (INTELEC), Scottsdale, AZ, USA, 30 September–4 October 2012.
15. Buja, G.; Bertoluzzo, M.; Mude, K.N. Design and Experimentation of WPT Charger for Electric City Car. *IEEE Trans. Ind. Electron.* **2015**, *12*, 7436–7447. [[CrossRef](#)]
16. Fu, M.; Yin, H.; Zhu, X.; Ma, C. Analysis and tracking of optimal load in wireless power transfer systems. *IEEE Trans. Power Electron.* **2015**, *30*, 3952–3963. [[CrossRef](#)]
17. Stoecklin, S.; Volk, T.; Yousaf, A.; Reindl, L. A Maximum Efficiency Point Tracking System for Wireless Powering of Biomedical Implants. *Procedia Eng.* **2015**, *120*, 451–454. [[CrossRef](#)]
18. Stoecklin, S.; Yousaf, A.; Volk, T.; Reindl, L. Efficient Wireless Powering of Biomedical Sensor Systems for Multichannel Brain Implants. *IEEE Trans. Instrum. Meas.* **2016**, *65*, 754–764. [[CrossRef](#)]
19. Li, H.; Li, J.; Wang, K.; Chen, W.; Yang, X. A maximum efficiency point tracking control scheme for wireless power transfer systems using magnetic resonant coupling. *IEEE Trans. Power Electron.* **2015**, *30*, 3998–4008. [[CrossRef](#)]
20. Diekhans, T.; De Doncker, R.W. A dual-side controlled inductive power transfer system optimized for large coupling factor variations. In Proceedings of the 2014 IEEE Energy Conversion Congress and Exposition (ECCE), Pittsburgh, PA, USA, 14–18 September 2014; pp. 652–659.
21. Erickson, R.W.; Maksimovic, D. *Fundamentals of Power Electronics*; Kluwer Academic Publishers: New York, NY, USA, 2001; pp. 712–713.

